Nitrogen addition using a gas blow in an ESR process

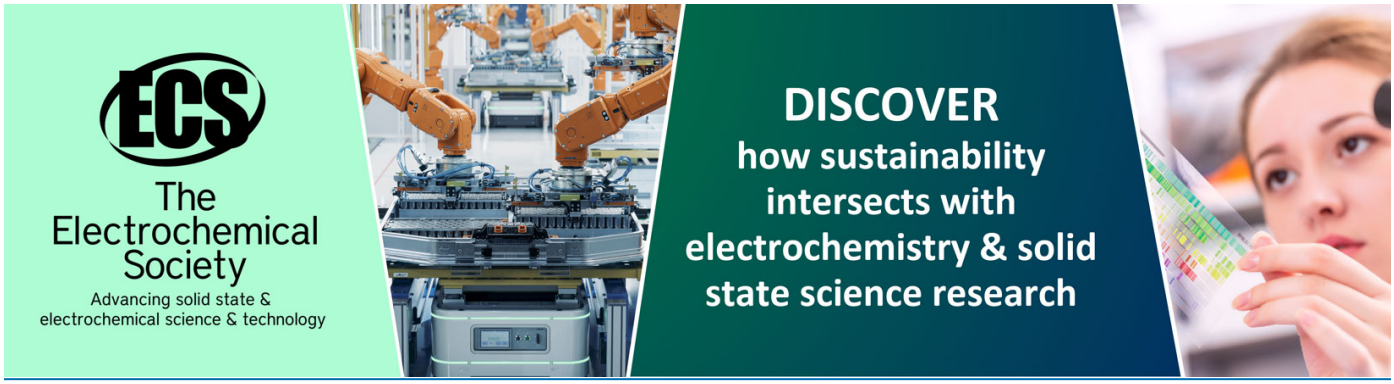

IOP Conf. Series: Materials Science and Engineering **143** (2016) 012005 doi:10.1088/1757-899X/143/1/012005

Nitrogen addition using a gas blow in an ESR process

S. Yamamoto[1], Y. Momoi[2], K. Kajikawa[2]

[1]Special Melting Shop, Material Manufacturing Department, Muroran Plant, The Japan Steel Works, Ltd., Japan

[2]Muroran Research Laboratory, Research and Development Headquarters, The Japan Steel Works, Ltd., Japan

suguru_yamamoto@jsw.co.jp, koji_kajikawa@jsw.co.jp

Abstract. A new nitrogen method for adding in an ESR process using nitrogen gas blown in through the electrode was investigated. Nitrogen gas blown through a center bore of the electrode enabled contact between the nitrogen gas and the molten steel directly underneath the electrode tip. A ϕ145mm diameter, laboratory-sized PESR furnace was used for the study on the reaction kinetics. Also, we carried out a water-model experiment in order to check the injection depth of the gas blown in the slag. The water model showed that the gas did not reach the upper surface of the molten metal and flowed on the bottom surface of the electrode only. An EPMA was carried out for a droplet remaining on the tip of the electrode after melting. The molten steel from the tip of the electrode shows that nitrogen gas absorption occurred at the tip of the electrode. The mass transfer coefficient was around 1.0×10^{-2} cm/sec in the system. This value is almost the same as the coefficient at the molten steel free surface.

1. Introduction

Nitrogen alloyed steels are widely used for drill collars, power-generation components, engine valves, high corrosion-resistance applications, bearings and other applications. Nitrogen alloying has two main benefits. One is strengthening owing to solid solution hardening [1], and the other is improvement of corrosion resistance[2]. Nitrogen-alloyed austenitic stainless steels less are likely to form processing evocation martensite. This enables the production of high-strength austenitic steel.

Several nitrogen addition methods have been developed in steel-making industries. Nitride addition is a popular method for high-nitrogen steel production. This method can increase the nitrogen content in steel effectively. However there is a disadvantage to this method. Nitride addition increases other elements such as Cr or Si. The gas-blow method is commonly used in a ladle furnace. This method has the advantage of eliminating contamination with other elements in nitride alloys. It is difficult to add nitrogen into a metal pool by blowing gas on the slag surface because steel-making slag has almost no nitrogen solubility. Direct contact between the nitrogen gas and the molten steel is required in order to add nitrogen using this method. Although bottom gas blowing can be used for nitrogen addition in a ladle furnace process, it cannot be applied to an electroslag remelting (ESR) process.

There is one solution for adding nitrogen in ESR. Prof. B. I. Medovar *et. al.* had developed Arc Slag Remelting (ASR)[3] as a method allowing direct contact between nitrogen gas and the molten steel in an ESR. However the heating method of ASR is different from that of a conventional ESR.

The electrode is not immersed in the slag and keeps some distance from slag surface in order to make a stable arc. Therefore ASR requires a special control system using feedback with respect to the current and arc voltage in order to stabilize the arc discharge.

A simpler way of nitrogen addition in ESR was investigated in this study. Gas blow through a center hole of the electrode was tried in an ordinary ESR melting condition. In this process, we may not need a special control system and could use a normal ESR control system. We confirmed how much nitrogen addition is possible by gas blow in a conventional ESR system.

2. Experimental procedure

Figure 1 shows the schematic of the experiment using a ϕ145mm mold pressurized electroslag remelting (P-ESR) furnace. A ϕ10mm hole was drilled through the center of the ϕ100mm electrode. Nitrogen gas was blown through the center hole to the electrode tip. The gas flow rate was 0.1-2.0 NL/min. The electrode material was SUS304 (AISI304, X5CrNi18-10) steel. The experimental conditions are shown in Table 1. The experiment was run under 0.98MPa pressurized and 0.1MPa atmosphere conditions. The melt voltage was 18V and the current was 2000A. In addition, a 20V-2500A melt was carried out for the 0.98MPa condition. After the ESR melt, the ingots were longitudinally cross-sectioned in order to perform macrostructure observation and chemical composition analysis. 20mm cubic samples for chemical analysis were taken at interval of 50mm from the bottom of the ingot.

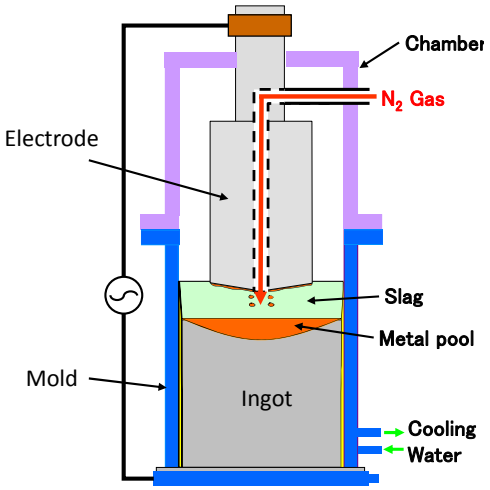

Figure1 Schematic of the Apparatus

Table 1 Experimental condition

	Atmosphere (MPa)	Voltage (V)	Current (A)	N_2 blow rate (NL/min)
Ingot 1	0.98	20	2500	0.2 – 0.8
Ingot 2		18 – 20	2000	1.0 – 2.0
Ingot 3	0.1	18		1

In order to confirm the blown gas immersion depth, a water-model experiment was also carried out. The same ϕ145mm mold P-ESR was used for this water model. A transparent plastic container was used for the water bath. It was placed under the electrode in substitution for the water-cooled coper mold. The bubble formation in water was observed from the side and the bottom of the container. The water model was run with gas blow rates of 0.8, 1.6, 3.1, 4.8, and 6.2 NL/min. There are some differences between the water-model and the actual ESR, such as the density of the liquid, the temperature and so on. The gas flow rate for the water-model experiment can be estimated from the modified Froude number Fr[4].

$$Fr = \frac{\rho_{g1} Q_{g1}^2}{\rho_{L1} g d_1^5} = \frac{\rho_{g2} Q_{g2}^2}{\rho_{L2} g d_2^5} \quad \cdots \quad (1)$$

where ρ_g is the gas density, Q_g is the gas flow rate, ρ_L is the density of the liquid, g is the standard acceleration due to gravity, and d is the diameter of the nozzle. Equation (1) becomes Equation (2).

$$Q_{g2} = \left(\frac{\rho_{g1} \rho_{L2}}{\rho_{g2} \rho_{L1}} \right)^{1/2} Q_{g1} \quad \cdots \quad (2)$$

The modified Froude number *Fr,* is a dimensionless number that represents the ratio between the forces of inertia and buoyancy. The blow distance can be dependent on the number. The blow rate in the water-model corresponds to blow rate in ϕ145mm SUS304 steel ESR at 1600°C of 0.5, 1.0, 1.8, 2.8, and 3.6 NL/min.

3. Result

The melt record of 20V-2000A melt is shown in Figure 2 as an example. The gas blow does little to disturb melting stability. The slag skin thicknesses of the test ingots were 0.5–3.0mm. The thickness values are the same as the ESR melt without gas blow. No clogging occurred in the center hole of the electrode tip after melt and gas blow was uninterrupted during the melt operation. For the blow rate of 0.2 to 1.0NL/min., the voltage swing and current swing value did not vary. However, when the blow rate increased to 2.0NL/min, the voltage and current swing became wider. 2.0NL/min. seemed maximum gas blow rate in the ESR furnace to perform stable melt with gas blow.

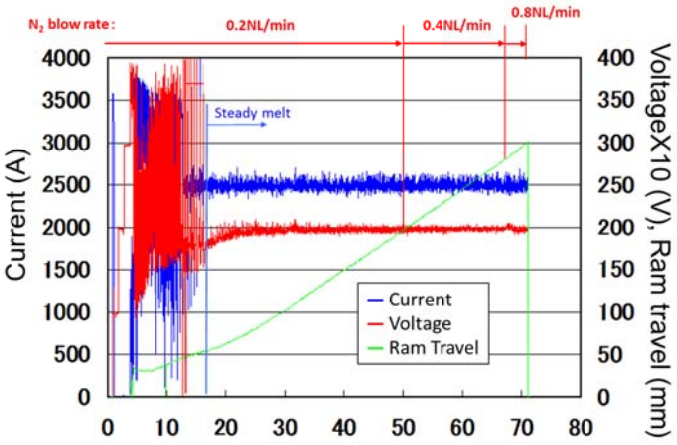

Figure 2 Melt record of Nitrogen blow ESR

The macrostructure of the ingot 1 is shown in Figure 3. An ingot melted without N_2 blow is also shown in the figure 3 for comparision. No structural disturbance was observed in the macrostructures. Inclined primary crystals grew from the bottom to the top. There was a slight solidification structure change at the point where the blow rate increased from 0.2NL/min to 0.4NL/min.

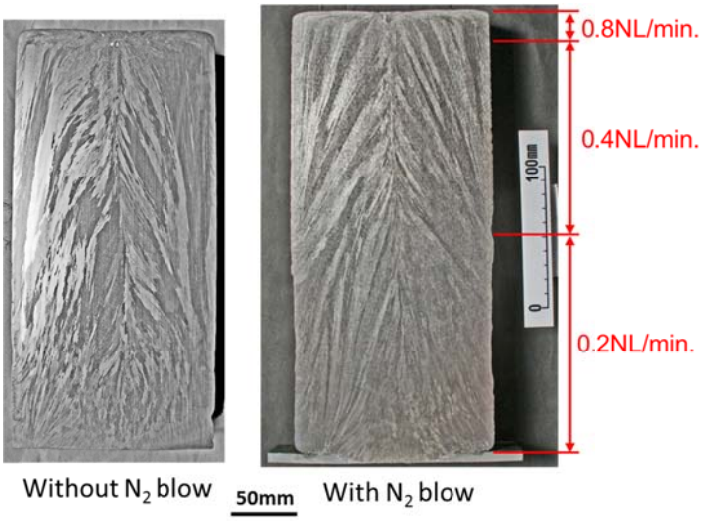

Figure 3 Macrostructure of the ingots

Table 2 shows the chemical composition in the middle of the ESR ingots and the electrodes. The nitrogen increment from the electrode to the ingots is shown in Figure 4. The values of the electrodes were plotted at 0 on the horizontal axis. All the ingots show addition of nitrogen. This figure indicates that nitrogen blowing through an electrode enables the addition of nitrogen into the steel in an ESR process.

In order to investigate the reaction site in this process, test specimens were clipped out from the electrode tip after the ESR melt and from the top of the ESR ingot. The tip of the remaining electrode

Table 2 Chemical composition of test ingots and electrodes (mass%)

	C	Si	Mn	P	S	Ni	Cr	Cu	Mo	V	Al	N*	O*
Electrode1	0.049	0.44	1.33	0.03	0.0250	7.91	17.96	0.45	0.32	0.06	<0.005	829	117
Ingot 1	0.051	0.41	1.32	0.03	0.0021	7.94	17.83	0.45	0.32	0.06	<0.005	1600	36
Electrode2	0.047	0.34	1.27	0.03	0.0220	7.90	18.44	0.38	0.25	0.08	0.010	636	216
Ingot 2	0.049	0.39	1.32	0.03	0.0017	8.04	18.21	0.49	0.30	0.06	<0.005	1910	40
Electrode3	0.048	0.32	1.27	0.03	0.0200	7.87	18.50	0.39	0.25	0.08	0.013	662	230
Ingot3	0.053	0.27	1.28	0.03	0.0017	8.04	18.44	0.40	0.26	0.08	<0.005	935	46

*ppm

was clipped out in order to confirm the reaction site of nitrogen absorption. Also a sample from the upper portion of the ingot was clipped out. Those samples were embedded in a resin EPMA mapping

analysis on the specimen as shown in Figure 5. The left side of the specimen is the top of the ingot and the right side is the tip of the electrode. In mapping for Ni, the columnar structure is shown on the right-hand side of the electrode. The microstrucure of the left-hand side of the electrode is different from that of the right-hand side. It can be considered that the left-hand side was melted in the ESR process. The N content in this melted portion is the same as that in the ingot. This indicates that the nitrogen absorption reaction in this process occurs at the molten metal film on the electrode.

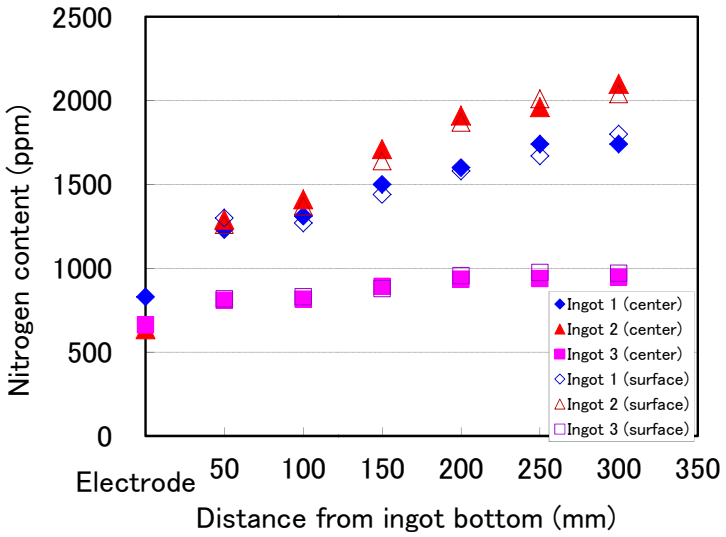

Figure 4 Chemical compositions in test ingots and electrodes

Figure 6 shows gas-bubble formation in the water model as observed from side views and bottom views of the electrode. The gas blow did not spurt out straight into water in all experimental conditions. The gas bubble formed just after the gas came out from the hole. The bubble did not go down because of the buoyancy force and grew underneath the electrode tip. After the bubble reached a certain size, it slid to one side of the electrode and detached from the tip.

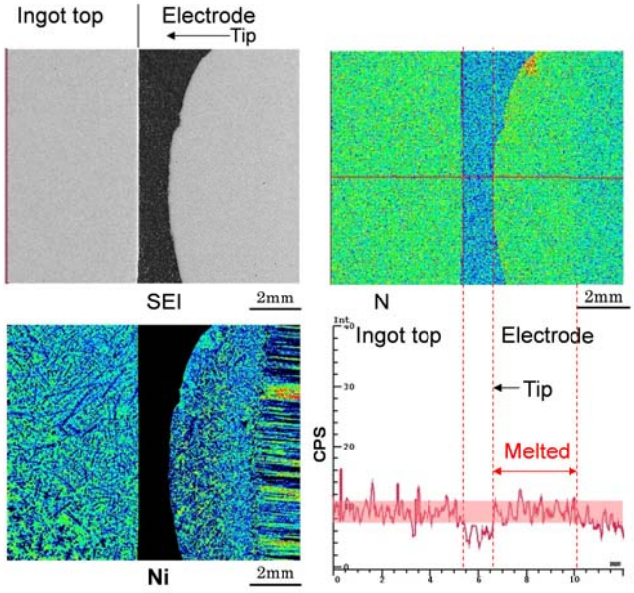

Figure 5 EPMA mapping analysis on the tip of electrode

The relationship between gas blow rate and maximum immersion depth of gas bubble is shown in Figure 7. The maximum immersion depth was around 4.5mm and almost constant for gas blow rates under 4.8NL/min. The maximum immersion depth was about 6.6mm with a blow rate of 6.2NL/min. Nitrogen blow rates in this experiment lower than 2.0NL/min. correspond to rate lower than 3.4NL/min in the water model. The slag weight was 2.2kg. From the slag weight, the slag cap height can be calculated as 50mm. The gas immersion depths around 5mm were much shallower than that of the slag cap height. It is considered that the blown nitrogen bubble did not reach the metal pool interface in this test melt condition.

Direct gas contact with the metal pool surface could not occur in the experimental condition. This observation indicates that this process is different from the one in ASR. Figure 8 shows the time history of the gas bubble projected surface area observation from the bottom of the electrode. The area increased with time and the bubble size reached a certain size. Then the bubble detached from the electrode and a new bubble started to grow again. For each blow rate, the surface area of the gas bubble increased with time in a roughly linear fashion.

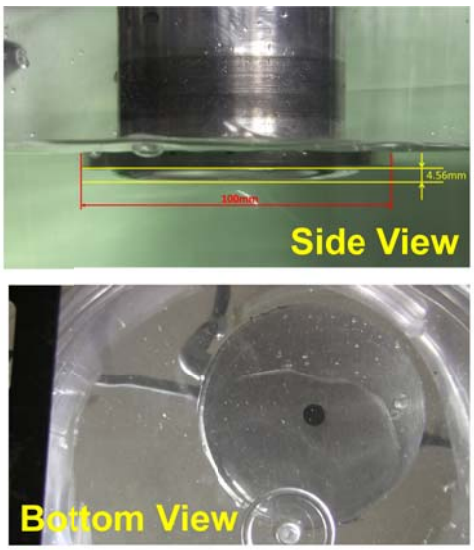

Figure 6 Bubble formations in water model

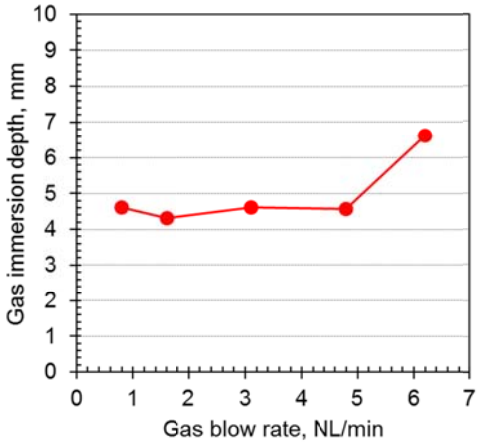

Figure 7 Gas immersion depths in water model

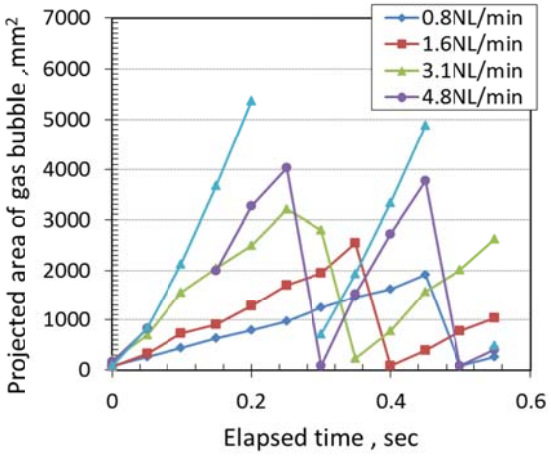

Figure 8 Time history of gas bubble projected area

4. Discussion

The apparent mass transfer coefficient was estimated for the gas-absorption reaction under nitrogen-gas blow in the ϕ145mm. P-ESR. The assumed condition for calculation is described here.

(1) The nitrogen-absorption reaction occurs at the molten metal film on the electrode tip. The nitrogen content in the metal droplet remained on the electrode bottom after the ESR. Therefore, it is considered that the nitrogen absorption reaction in this process occurred at the molten metal film on the bottom of the electrode.

(2) The nitrogen-absorption reaction mass transfer rate is limited at the metal side. It obeys the rule of a primary reaction[4].

$$-\frac{dC}{dt} = k_{metal}(\frac{A}{V})(C - C_i) \quad \cdots \quad (3)$$

Equation (3) becomes

$$-\ln(\frac{C - C_{eq}}{C_0 - C_{eq}}) = k_{metal}(\frac{A}{V})t \quad \cdots \quad (4)$$

Where, C is the nitrogen content in the metal, C_i is the nitrogen content at the gas-metal interface, C_{eq} is the equilibrium nitrogen content for each partial pressure, C_0 is the nitrogen content in the metal before nitrogen absorption, t is the reaction time, A is the interfacial area of the metal for reaction, V is the volume of metal for reaction, and k_{metal} is the apparent mass transfer coefficient.

(3) Slag cap/metal pool interfacial temperature at each ingot height

This value was assumed from the Al deoxidation equilibrium value in carbon steel from other experiments using the ϕ145mm. P-ESR.

2000A-20V condition : T = -0.5112d + 1868.2

2500A-20V condition : T = -0.3391d + 1866.3

Where, d is the distance from the ingot bottom, and T is the slag cap/metal pool interfacial temperature at distance d from ingot bottom.

(4) The temperature vicinity of the electrode bottom (molten metal film)/slag cap for each ingot height is assumed as the slag cap/metal pool interfacial temperature -250°C. This follows the measured slag cap temperature distribution in the ϕ180mm ESR[6].

(5) Metal volume for reaction

This is the volume of molten metal film under the electrode tip. The thickness is assumed as 1mm and the film covered the whole bottom surface of the electrode. This was expected from the EPMA analysis of the electrode tip as shown in Figure 5.

(6) Interfacial area of metal for reaction

This is the average contact area between the nitrogen gas bubble and the molten metal film. The result of the water model is used for this value.

Figure 9 shows the relationship between the distance from the ingot bottom and the apparent mass transfer coefficient k_{metal} for the nitrogen absorption reaction. k_{metal} increases from the bottom to the top of the ingot in either condition. However the increment is not significant and the apparent mass transfer coefficient for the nitrogen absorption reaction did not depend on the ESR ingot height significantly. The value is around 1.0×10^{-2}cm/sec.

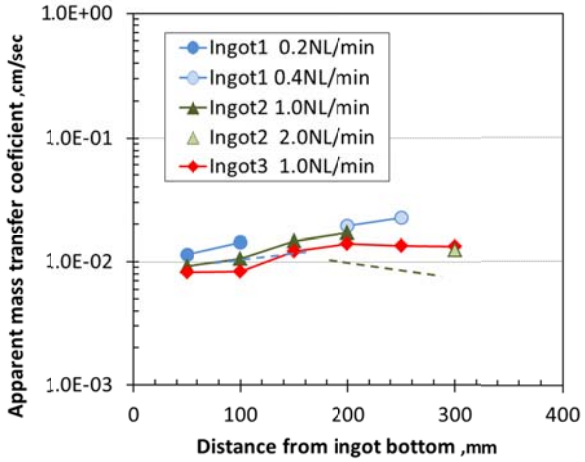

Figure 9 Relationship between distance from ingot bottom and apparent mass transfer coefficient

Table 3 shows the apparent mass transfer coefficients of the nitrogen absorption reaction for the Fe, Fe-Cr, and Fe-Cr-Ni systems at 1600°C[7-11]. These values are for reactions measured at the free surface of the molten steel. The k_{metal} value estimated from this experiment is also given in Table 3. The k_{metal} values estimated from this experiment are consistent with the value reported by Fedorchenko[9]. The estimated value is within the range of the reported values. Nitrogen absorption rates in the longitudinal direction of the ingot could be constant since the k_{metal} values are almost constant as shown in Figure 9. The transition of the nitrogen contents in the ingots are shown in Figure 10. The equilibrium nitrogen contents for each location are also plotted in this figure. These equilibrium nitrogen contents are calculated from the estimated temperature vicinity of the electrode bottom/slag pool. Both nitrogen contents and equilibrium nitrogen contents increased from the bottom to the top of the ingot. Longitudinal variation in the nitrogen contents of the ESR ingots could be due to equilibrium nitrogen contents with metal temperature change in the vicinity of the slag/molten metal film interface. In case of small size ESR such as this apparatus, it may difficult to obtain constant slag temperature. However if the furnace size becomes larger, the temperature change becomes milder. It could be available to obtain near constant temperature condition in a large sized commercial ESR and to make much uniform nitrogen content.

Table 3 Mass transfer coefficients of Nitrogen absorption reaction

	Alloy type	k_{metal}
Chou [7]	Fe	0.0345
	Fe-18Cr	0.0342
Pehlke [8]	Fe-20Cr	0.022
Fedorchenko [9]	Fe-18Cr	0.014
	Fe-18Cr-10Ni	0.012
Gruszcyk [10]	PN-88	0.0065
Takahashi [11]	Fe-10Cr	0.0088*
Present Work	Fe-18Cr-8Ni	0.0103

*) 1823K

5. Conclusion

Nitrogen addition by gas blow through a center hole of an electrode was tried with ordinary ESR melting conditions.

・ Nitrogen addition by nitrogen gas is possible in a ordinary ESR system using gas blow through an electrode.

・Blown gas from center of the electrode could not penetrate through the slag. There was no direct gas contact on the metal pool surface in the experimental condition.

・The mass transfer coefficient for the nitrogen absorption rate was around $1x10^{-2}$ cm/sec.

・Longitudinal variation in the nitrogen contents of the ESR ingots could be due to equilibrium nitrogen contents with metal temperature change in the vicinity of the slag/molten metal film interface.

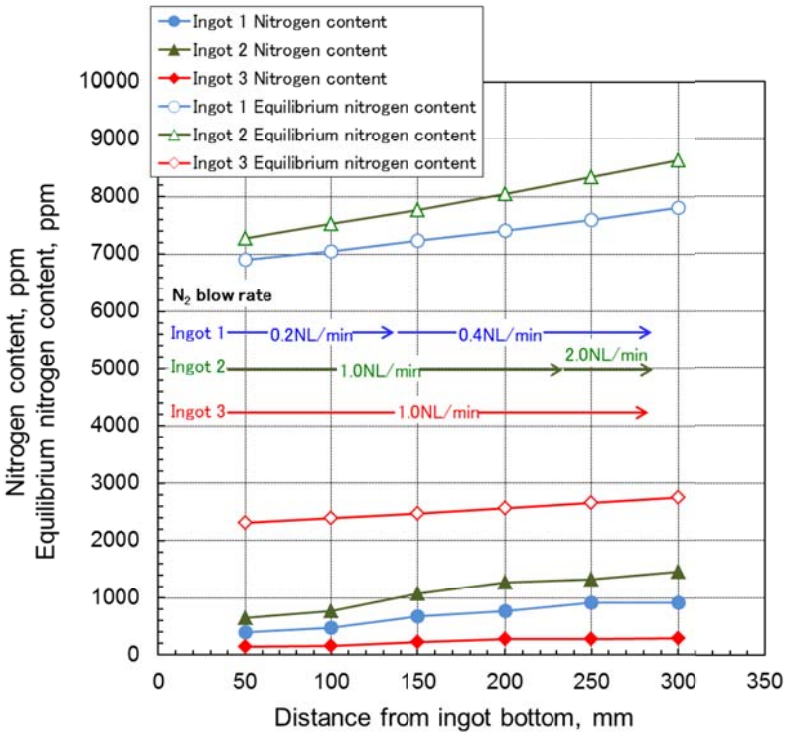

Figure 10 Comparison between nitrogen content and equilibrium nitrogen content calculated from chemical composition.

6. Acknowledgments

We greatly thank Prof. Alec Mitchell of the University of British Columbia for useful discussion.

References

[1] P. G. Uggoweizer and M. Harzermoser: High Nitrogen Steel (1988) p. 174
[2] S. Azuma, H. Miyuki, and T. Kudo: ISIJ int., 36(1996) p.793
[3] B. I. Medovar, V. Ya. Saenko, G. M. Grigorenko, Yu. M. Pomarin, and V. I. Kumysh: "Arc-Slag Remelting of Steel and Alloys", (1996) Cambridge International Science Publishing.
[4] M. Byrne and G. R. Belton: Metall. Trans. B, 14B(1983) P.441
[5] K. Amano ,K. Ito and H. Sakao: Tetsu-to-Hagane, 62(1976) p.1179
[6] M. Kawakami, K. Nagata, M. Yamamura, N. Sakata, Y. Miyashita, and K. Goto: Tetsu-to-Hagane, 63(1977) No.13, p.2162
[7] T. Choh, T. Yamada, and M. Inoue:Tetsu-to-Hagane, 62(1976) No.3, p334
[8] R. D. Pehlke and J. F. Elliott: Trans. Met. Soc. AIME, 227(1963), p.884
[9] V.I. Fedorchenko V. V. Averin: The Forth Japan-USSR Joint Symposium Physical Chemistry of Metallurgical Process, (1973) p.167
[10] A. Gruszcyk: J. of Achiev. in Manuf. Eng. 26(2008) p.115
[11] F. Takahashi, Y. Momoi, K. Kajikawa, and H. Yamada: Tetsu-to-Hagane, 97(2011) p.525
[12] W. P. Wu and D. Janke: Ironmaking Steelmaking, 23(1996) p.247